

# Effect of milling process on core-shell microstructure and electrical properties for BaTiO<sub>3</sub>-based Ni-MLCC

Youchi Mizuno \*, Tomoya Hagiwara, Hirokazu Chazono, Hiroshi Kishi

*Taiyo Yuden Co., Ltd., 5607-2 Nakamuroda Haruna-machi, Gunma-gun, Gunma 370-3347, Japan*

Received 4 September 2000; received in revised form 23 October 2000; accepted 30 October 2000

## Abstract

The effect of the process parameter in the milling process on the microstructural evolution and the electrical properties of multilayer ceramic capacitor (MLCC) samples were investigated in the BaTiO<sub>3</sub> (BT)–Ho<sub>2</sub>O<sub>3</sub>–MgO system. The microstructure for MLCC samples fired at 1320°C was dependent on the degree of damage for BT given by the milling process, judging from the field emission scanning electron microscopy observation and differential scanning calorimetry measurement (DSC). The mean grain size ( $D_{50}$ ) determined from the chemically etched samples decreased as the damage increased. The endothermic peak of DSC profile at around 125°C was broadened and the peak area decreased as the damage increased. Furthermore, the electrical properties were dependent on the degree of damage. The dielectric constant for MLCC samples decreased and the peak of dielectric constant at around room temperature shifted to a higher temperature as the damage increased. It was found that the MLCC sample showed the small leakage current and long mean lifetime as the degree of damage increased. © 2001 Elsevier Science Ltd. All rights reserved.

**Keywords:** BaTiO<sub>3</sub> and titanates; Capacitors; Electrical properties; Microstructure-final; Milling

## 1. Introduction

Recent progresses in technology for fabricating MLCCs have been compelled by the down sizing and cost reduction. In order to meet these stringent requirements, the number of the dielectric active layers was increased, and the thickness was decreased, without compromising product reliability. Furthermore, the noble metal (Pd) is replaced by the base metal (Ni) as the internal electrode material to lower the production cost. A deliberate design of the microstructure for individual grains must be essential for such MLCCs with considerably thin dielectric layers since the microstructure has a decisive influence on the electrical properties and reliability of the MLCCs.<sup>1–3</sup>

Previously, we have reported that the given damage on BT by the milling process has a fatal influence on the microstructure and the rate of frequency for grains showing the core-shell microstructure increased as the damage increased for disk samples, judging from the statistical analysis by the transmission electron microscopy (TEM).<sup>4</sup>

In this study the microstructure of MLCC samples was compared with that of disk samples first, and the relationship between the microstructural evolution caused by the damage on BT by the milling process and the electrical properties for MLCC samples were investigated in the BT–Ho<sub>2</sub>O<sub>3</sub>–MgO system.

## 2. Experimental

### 2.1. Sample preparation

BT, reagent-grade MgO, Ho<sub>2</sub>O<sub>3</sub>, MnO, and BaSiO<sub>3</sub> were weighed in following composition: 1.000BT + 0.005 = MgO + 0.010Ho<sub>2</sub>O<sub>3</sub> + 0.001MnO + 0.015BaSiO<sub>3</sub>. BT was synthesized hydrothermally and was heat-treated to grow into a mean particle diameter of about 0.5 μm (SAKAI Chemical Industry Co., Ltd.). BaSiO<sub>3</sub> was used as a sintering aid. They were mixed by ball milling for 15 h. The degree of damage for BT powder was controlled by the amount of the milling medium. The weight of medium used in a milling process was equal to that of BT for the sample-1, and was twice and four times as heavy as BT for the sample-2 and sample-3, respectively. The powder mixtures were subsequently dried and sieved.

\* Corresponding author. Tel.: +81-27-360-8307; fax: +81-27-360-8315.

E-mail address: ymizuno@jty.yuden.co.jp (Y. Mizuno).

MLCC samples were prepared by the following procedure. The obtained powders and an appropriate organic binder were dispersed into a slurry. Then green sheets with the thickness of 5  $\mu\text{m}$  were formed by the so-called doctor-blade method. After Ni internal electrodes were printed on these green sheets, they were laminated and pressed into a bar with 10 dielectric layers and cut into pieces. After burning out the binder, they were fired at 1320°C for 2 h and cooled to 1000°C in a reducing atmosphere controlled by  $\text{H}_2$ ,  $\text{N}_2$ ,  $\text{O}_2$ , and  $\text{H}_2\text{O}$ , then to room temperature in a weakly oxidizing atmosphere ( $\text{P}(\text{O}_2) = 30$  Pa at 1000°C).

## 2.2. Characterization

The degree of damage given by milling process for BT powder was defined as the ratio of the full-width at half maximum (FWHM) in XRD analysis as described in a previous paper.<sup>4</sup> The chemically etched surface for MLCC samples were observed by the field emission scanning electron microscopy (FE-SEM) to investigate the microstructural changes. The grain diameter was measured for more than 500 grains by the intercept method and the mean grain size ( $D_{50}$ ) was defined as the grain diameter giving 50% of the accumulated volume. The phase transition of the sintered samples was characterized by DSC measurement in order to obtain the information only from the core region, since the core is composed of pure BT.<sup>5</sup>

Table 1  
Powder features

	$D_{50}$ ( $\mu\text{m}$ )	BET ( $\text{m}^2/\text{g}$ )	FWHM ( $^\circ$ )
Raw BT	0.500	(2.40)	0.1036
Sample-1	0.508	3.53	0.1080
Sample-2	0.489	3.71	0.1113
Sample-3	0.479	4.40	0.1224

The capacitance and dissipation factor ( $\tan\delta$ ) for the MLCC samples, which had been treated thermally at 150°C for 1 h, were measured using an LCR meter (HP4284A) at 1 kHz 1 Vrms on heating from –55 to 150°C. A highly accelerated life test (HALT) of insulation resistance (IR) was conducted at 150°C under applied voltage of 20 V/ $\mu\text{m}$ .

## 3. Results and discussion

### 3.1. Microstructural evolution

We previously reported that the increase in the amount of milling medium brought about the chipped particles of BT powders and the decrease of the BT crystallinity as shown in Table 1. Furthermore, careful TEM observation revealed that there were grains without 90° domain pattern (named S-grain) and grains showing only 90° domain pattern (named C-grain), as well as grains showing core-shell microstructure (named CS-grain) for disk samples as shown in Fig. 1.<sup>4</sup> The rate of frequency for three kinds of grains was summarized in Table 2. The rate of frequency for CS-grain increased, and that for C-grain decreased as the damage increased. It is important to investigate that the microstructure of MLCC samples is similar to that of disk samples or not. So the microstructure of MLCC samples was compared with that of disk samples first. Figs. 2 and 3 showed SEM micrographs and the grain size distributions for MLCC samples, respectively, fired at 1320°C determined from the chemically etched surface. Only the grains between the internal electrodes were measured and treated statistically. The profiles of the curve were similar for all samples and  $D_{50}$  decreased as the degree of damage increased.  $D_{50}$  was almost equal to that of the disk samples as shown in Table 3. Therefore, little grain growth was also occurred for all MLCC samples, which was similar to the case of disk samples.

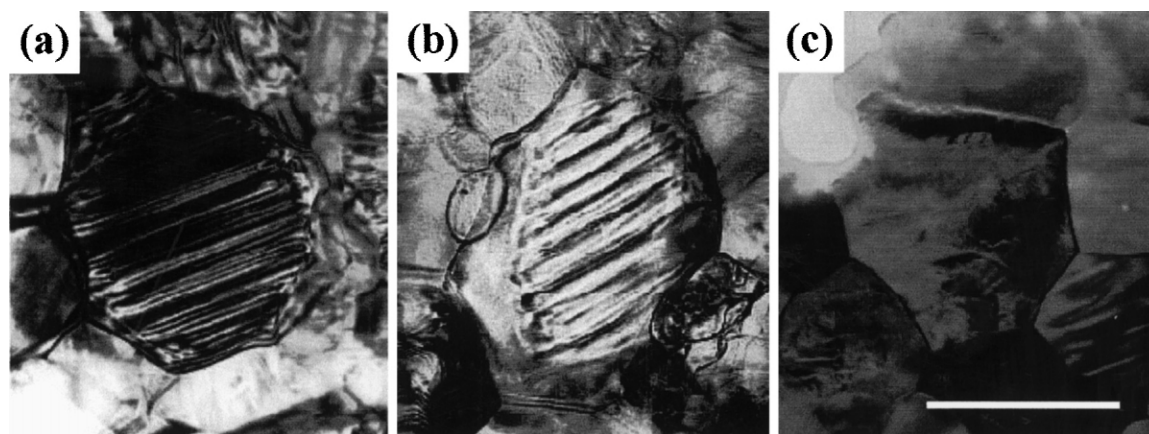


Fig. 1. The typical TEM micrographs for disk samples: (a) is the C-grains; (b) is the CS-grains (c) is the S-grains (bar = 0.5  $\mu\text{m}$ ).

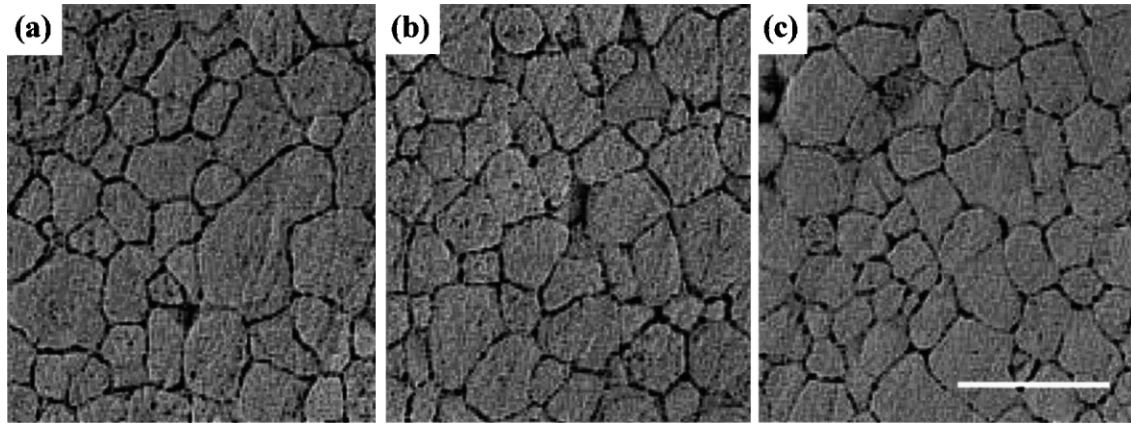


Fig. 2. The typical FE-SEM micrographs of chemically etched MLCC sample surfaces: (a) is the sample-1; (b) is the sample-2; (c) is the sample-3 (bar = 1.0  $\mu\text{m}$ ).

Table 2

The rate of frequency for C-grain, CS-grains, and S-grains for disk samples

	C-grain (%)	CS-grain (%)	S-grain (%)
Sample-1	50	46	4
Sample-2	48	45	7
Sample-3	23	70	7

Table 3

Comparisons between the mean grain size for fired MLCC samples and that for disk samples

	$D_{50}$ ( $\mu\text{m}$ ) MLCC	$D_{50}$ ( $\mu\text{m}$ ) disk
Sample-1	0.502	0.507
Sample-2	0.478	0.497
Sample-3	0.475	0.474

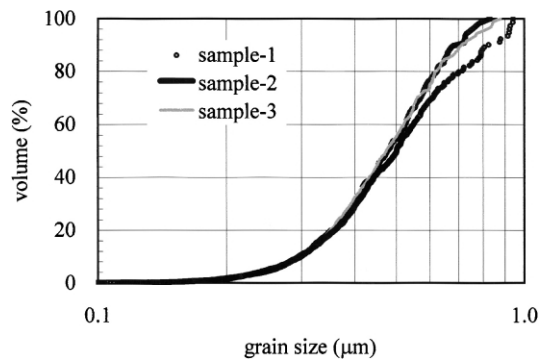


Fig. 3. The grain size distribution determined from the chemically etched surface of the sample fired at 1320°C.

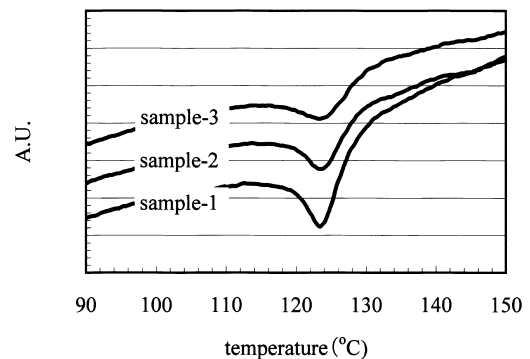


Fig. 4. DSC profiles of MLCC samples fired at 1320°C.

The DSC profiles for MLCC samples were almost equal to that of disk samples as shown in Fig. 4. The peak was broadened and the peak area decreased as the damage became heavier, whereas the peak temperature was almost independent on the degree of damage. The change of the peak profile must be conjunction with the core volume and the presence of the internal stress in samples composed of the core-shell microstructure.<sup>6</sup> The results of DSC measurement for MLCC samples were almost equal to that of disk samples as summarized in Table 4. Therefore, it was found that the rate of frequency for CS-grains and the shell region increased similarly as the damage increased for MLCC samples, judging from SEM observation and DSC measurement.

### 3.2. Electrical properties

It was found that the microstructure for MLCC samples was dependent on the degree of damage given by the milling process. The electrical properties, temperature characteristics of dielectric constant and  $\tan\delta$  were measured next. The dielectric constant for MLCC samples with 3.5  $\mu\text{m}$  dielectric thickness decreased monotonically with the degree of damage increased in all the measuring temperature range as shown in Fig. 5. Furthermore, the peak of dielectric constant at around room temperature shifted to a higher temperature as the damage increased. Arlt has reported that dielectric constant decreased with decreasing grain size for pure BT in the grain size range of below 0.7  $\mu\text{m}$ .<sup>7</sup> It was suggested that the decrease of dielectric

Table 4  
DSC peak temperature and its peak area

	Peak temperature (°C)		Peak area (mcal/g)	
	Disk	MLCC	Disk	MLCC
Sample-1	124.0	123.4	100.0	107.8
Sample-2	124.2	123.3	86.7	69.2
Sample-3	123.6	123.2	75.1	53.4

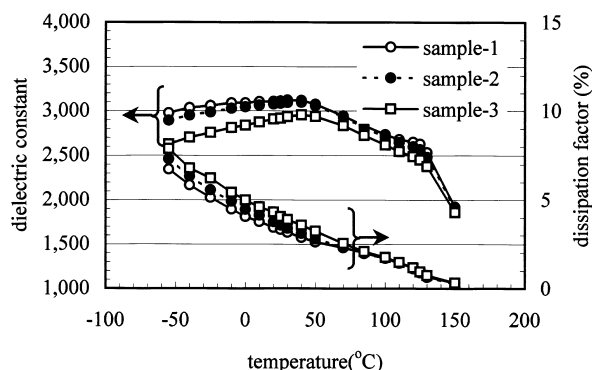


Fig. 5. The dielectric constant and the dissipation factor for MLCC samples as a function of temperature.

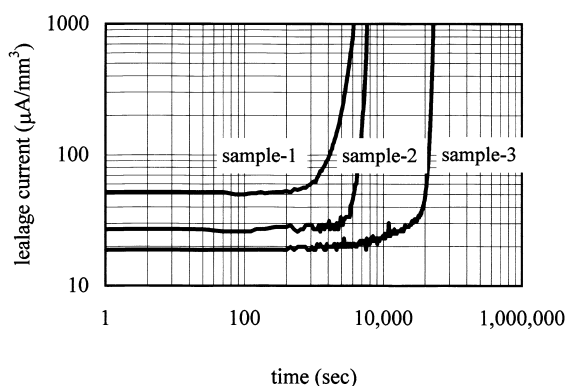


Fig. 6. Typical data of the time dependence of leakage current for MLCC samples at 150°C under 20 V/μm.

constant with increasing damage was caused by the volumetric decrease of core region composed of pure BT. On the other hand, the  $\tan\delta$  increased as the damage given by milling process increased. It seemed that there was an intimate relationship between  $\tan\delta$  and the peak of dielectric constant.

HALT was conducted on 20 MLCC samples and the only profiles with the mean time to failure (MTTF) were plotted in Fig. 6. The leakage current decreased and the lifetime was prolonged as the degree of damage increased. It was suggested that the volumetric ratio of the shell region influenced the load lifetime characteristics of MLCC samples.

These findings indicated that electrical properties were strikingly affected by the microstructural evolution. Further investigation of the physical and chemical properties such as the compositional distribution in the shell region, is necessary to elucidate the relationship between the microstructural evolution and electrical properties.

## References

1. Mizuno, Y., Okino, Y., Kohzu, N., Chazono, H. and Kishi, H., Influence of the microstructure evolution on electrical properties of multilayer capacitors with Ni electrode. *Jpn. J. Appl. Phys.*, 1998, **37**, 5227–5231.
2. Okino, Y., Kohzu, N., Mizuno, Y., Honda, M., Chazono, H. and Kishi, H., Effects of the microstructure on dielectric properties for BaTiO<sub>3</sub>-based MLC with Ni electrode. *Key Engineering Materials*, 1999, **157**, 9–15.
3. Chazono, H., Okino, Y., Kohzu, N. and Kishi, H., Effect of Sm and Ho addition on the microstructure and electrical properties in MLCC with Ni internal electrode. *Ceramic Transactions*, 1999, **97**, 53–64.
4. Mizuno, Y., Hagiwara, T., Chazono, H. and Kishi, H., Effect of milling process on core-shell microstructure for BaTiO<sub>3</sub>-based Ni-MLCC, submitted to *Am. Ceram. Soc.*
5. Saito, H., Chazono, H., Kishi, H. and Yamaoka, N., X7R multilayer ceramic capacitor with nickel electrodes. *Jpn. J. Appl. Phys.*, 1991, **30**, 2307–2310.
6. Armstrong, T. R. and Buchanan, R. C., Influence of core-shell grains on the internal stress state and permittivity response of zirconia-modified barium titanate. *J. Am. Ceram. Soc.*, 1990, **73**(5), 1268–1273.
7. Arlt, G., The influence of microstructure on the properties of ferroelectric ceramics. *Ferroelectrics*, 1990, **104**, 217–227.